Inhibition of viral group-1 and group-2 neuraminidases by oseltamivir: A comparative structural analysis by the ScrewFit algorithm

Paolo A. Calligari [a,b,c,*], Gerald R. Kneller [a,d,e], Andrea Giansanti [f], Paolo Ascenzi [g,h], Alessandro Porrello [i], Alessio Bocedi [h,*]

[a] Centre de Biophysique Moléculaire, CNRS UPR 4301, Rue Charles Sadron, F-45071 Orléans Cedex 2, France
[b] Institut Laue-Langevin, 6 Rue Jules Horowitz BP 156, F-38042 Grenoble Cedex, France
[c] Laboratoire Léon Brillouin, CNRS UMR 12, F-91191 Gif-sur-Yvette, France
[d] Université d'Orléans, Château de la Source — Avenue du Parc Floral, F-45067 Orléans, France
[e] Synchroton SOLEIL, Saint Aubin BP48, F-91192 Gif-sur-Yvette Cedex, France
[f] Dipartimento di Fisica, Università Roma La Sapienza, Piazzale Aldo Moro 5, I-00185 Roma, Italy
[g] Istituto Nazionale per le Malattie Infettive IRCCS 'Lazzaro Spallanzani', Via Portuense 292, I-00149 Roma, Italy
[h] Laboratorio Interdipartimentale di Microscopia Elettronica, Università Roma Tre, Via della Vasca Navale 79, I-00146 Roma, Italy
[i] Institute for Genome Sciences and Policy, Duke University, 101 Science Drive, Durham, NC 27708, USA

ARTICLE INFO

ABSTRACT

The viral surface glycoprotein neuraminidase (NA) allows the influenza virus penetration and the egress of virions. NAs are classified as A, B, and C. Type-A NAs from influenza virus are subdivided into two phylogenetically distinct families, group-1 and group-2. NA inhibition by oseltamivir represents a therapeutic approach against the avian influenza virus H5N1. Here, structural bases for oseltamivir recognition by group-1 NA1, NA8 and group-2 NA9 are highlighted by the ScrewFit algorithm for quantitative structure comparison. Oseltamivir binding to NA1 and NA8 affects the geometry of Glu119 and of regions Arg130-Ser160, Val240-Gly260, and Asp330-Glu382, leading to multiple NA conformations. Additionally, although NA1 and NA9 share almost the same oseltamivir-bound final conformation, they show some relevant differences as suggested by the ScrewFit algorithm. These results indicate that the design of new NA inhibitors should take into account these family-specific effects induced on the whole structure of NAs.

© 2009 Elsevier B.V. All rights reserved.

Influenza (flu) is a serious respiratory illness with annual epidemics (see: http://www.who.int/csr/disease/influenza/en/). Flu viruses, belonging to the *Orthomyxoviridae* family, are classified as A, B, and C, on the basis of the antigenic differences of their nuclear and matrix proteins,; all avian flu viruses belong to type-A. The antigenicity of the two surface glycoproteins hemagglutinin (H) and neuraminidase (NA) is used to cluster type-A flu viruses into subtypes: 16 for H (H1–H16) and 9 for NA (NA1–NA9). Virus uptake to the cell-surface sialic acid receptor is mediated by H. After virus replication, NA removes sialic acid from viral and cellular glycoproteins to facilitate virus release. Different combinations of H and NA subtypes (*i.e.*, H*x*N*y*) have been found in avian species [1–3].

The possible transmission of mutant viruses of avian flu to humans indicate that the danger of a pandemic is real, thus urging the scientific community to develop new anti-flu drugs, able to respond to the repertoire of antigenic mutations in the H5N1 virus strains [1–3].

Two classes of antiviral drugs are available against flu viruses: the inhibitors of the ion channel activity of the M2 membrane protein (*i.e.*, amantadine and rimantadine), and the NA inhibitors (*i.e.*, oseltamivir (Tamiflu®) and zanamivir (Relenza®)). The resistance against both oseltamivir and zanamivir reflects single point mutations of highly conserved NA residues [4,5]. Specifically, the sensitivity of flu viruses to oseltamivir, expressed by inhibition of the NA activity (IC_{50}), is different between oseltamivir-sensitive viruses ($IC_{50} \cong 0.1$–10 nM), and drug-resistant viruses ($IC_{50} \cong 90$ nM) [6].

NAs are homo-tetrameric glycoproteins of ~240 kDa belonging to the three different types A, B, and C. Type-A NAs are subdivided in two phylogenetically distinct groups. Group-1 contains NA1, NA4, NA5, and NA8, whereas group-2 comprises NA2, NA3, NA6, NA7, and NA9 [7]. Notably, NA2 and NA9 have been used to design selective NA inhibitors oseltamivir and zanamivir [7].

Here, a detailed comparative analysis of the three-dimensional structures of oseltamivir-free and oseltamivir-bound viral NA1, NA8, and NA9 by the ScrewFit algorithm is reported. The latter represents a

new quantitative approach for structure comparison based on the analysis of the screw motions of contiguous peptide planes along a protein backbone [8–10].

Finally, we show that the ScrewFit analysis of NAs structures confirm most of the recent experimental results in respect to the differences between group-1 and group-2 NAs [11]. In particular, we show that the ligand-free NA1 conformation is very similar to the oseltamivir-complexed NA1 open conformation whereas the closed ligand-bound conformation shows some relevant differences from them. We also display that these differences are group-dependent as they are also shown by the same comparison for NA8 conformations (group-1) but not in NA9 ones (group-2). This result is coherent to the fact that oseltamivir has been designed using group-2 NAs as templates [7].

Interestingly, the three-dimensional structure of the NA1 oseltamivir-bound closed conformation and NA9 are very similar, excepting some differences not reported in previous studies [11] and detected here by means of ScrewFit. These results indicate that NA inhibitors should be designed expressly taking the target enzyme as the template; in this way cross-inhibition of group-1 and group-2 NAs could not be excluded, resulting less efficacy by a effective therapeutically point of view.

1. Materials and methods

1.1. Sequence analysis of NAs

The amino acid sequences of NAs from flu type-A viruses NA1 (PDB id: 2HTY), NA2 (PDB id: 2BAT), NA3 (NCBI id: AAO62020.1), NA4 (PDB id: 2HTV), NA5 (NCBI id: AAA43672.1), NA6 (PDB id: 1V0Z), NA7 (NCBI id: AAA43425.1), NA8 (PDB id: 2HT5), and NA9 (PDB id: 7NN9), and from the flu type-B virus (PDB id: 1INF) were recovered from the NCBI database (available at: http://www.ncbi.nlm.nih.gov), and from the Protein Data Bank [12]. The amino acid sequences have been multi-aligned with ClustalW (available at: http://www.ebi.ac.uk) (Fig. S1). The amino acid residue numbering adopted here corresponds to that reported by Russell and coworkers [11].

1.2. ScrewFit analysis of NA three-dimensional structures

The three-dimensional structures used in the ScrewFit analysis were obtained from the Protein Data Bank [12]: NA1 (ligand-free, PDB id: 2HTY; oseltamivir-bound open conformation, PDB id: 2HU0; oseltamivir-bound closed conformation, PDB id: 2HU4) [11], NA8 (ligand-free, PDB id: 2HT5, oseltamivir-bound 'open' conformation, PDB id: 2HT7; oseltamivir-bound 'closed' conformation, PDB id: 2HT8) [11], and NA9 (ligand-free, PDB id: 7NN9) [13]; oseltamivir-bound conformation (PDB id: 2QWK) [14]) (Fig. S2). The analysis is just limited to these structures for a better comprehension of the relationships among proteins belonging to type-A and -B NAs crystallized with the same compound (e.g., oseltamivir).

The ScrewFit algorithm [8,9] superposes molecular structures, defined by atomic coordinates, combining quaternionic representation of rotation matrices and Chasles' theorem on rigid-body displacements. When applied to subsequent peptide planes in protein structures, ScrewFit gives local helical parameters of the protein backbone winding (see: http://dirac.cnrs-orleans.fr/Screwit/) [8–10].

The ScrewFit algorithm takes into consideration three structural parameters: the orientational distance, the radius of screw motion, and the straightness. For each pair of consecutive peptide planes represented by their atoms {C, O, N}, ScrewFit defines three parameters indicating their relative orientation and distance from a common axis of rotation (the axis of screw motion) (Fig. 1).

The oxygen, carbon, and nitrogen atoms can be used to define the plane of a peptide group. Two subsequent peptide planes can be
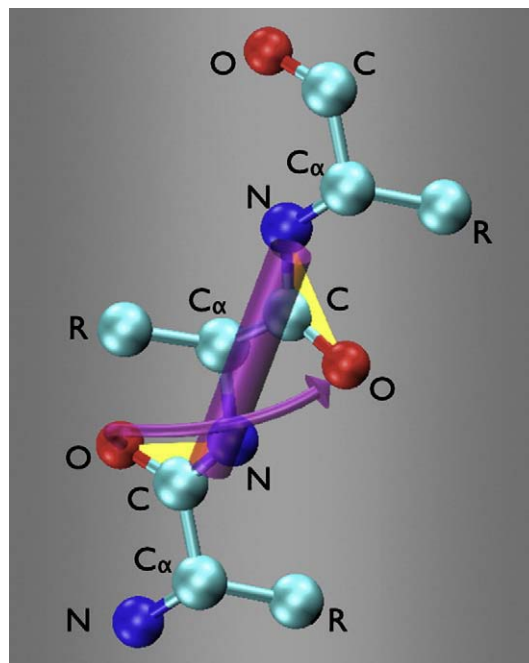

Fig. 1. A tri-peptide with two peptide bonds in the extended conformation, where the symbol "R" stands for a non-specified side-chains. The screw motion relating the yellow triangles formed by the {O, C, N} atoms of the peptide planes defines the local helix which is schematically represented by the cylinder and the corresponding screw arrow. The radius of the cylinder corresponds to the radius of the screw motion. At the same extent, the scalar product of the axis of two consecutive cylinders correspond to the straightness parameter. The orientational distance, which cannot be displayed in the figure, it refers to the relative orientation of the two subsequent peptide planes. (For interpretation of the references to color in this figure legend, the reader is referred to the web version of this article.)

superposed as rigid bodies, through the minimization of the target function

$$m(\boldsymbol{q}) = \sum_{\alpha=1}^{3} \omega_\alpha (\mathbf{D}(\boldsymbol{q}) \cdot x_\alpha - x'_\alpha)^2, \qquad (1)$$

where $\{x_\alpha\}$ and $\{x'_\alpha\}$ are the coordinates of the atoms in the reference and target plane, respectively. Both sets of coordinates are to be taken relative to the respective centers of rotation, which is here chosen to be the C-atom. The index α runs over the three atomic species {α=O, C, N} and to each atom is assigned a positive weight ω_α value proportional to its mass (with $\sum_{\alpha=1}^{3} \omega_\alpha = 1$). The vector $\boldsymbol{q} \equiv \{q_0, q_1, q_2, q_3\}$ comprises four real normalized quaternion components, with $q_0^2 + q_1^2 + q_2^2 + q_3^2 = 1$ and $\mathbf{D}$ is a proper rotation matrix, with det($\mathbf{D}$)=+1, which has the form

$$\mathbf{D} = \begin{pmatrix} q_0^2 + q_1^2 - q_2^2 - q_3^2 & 2(-q_0 q_3 + q_1 q_2) & 2(q_0 q_2 + q_1 q_3) \\ 2(q_0 q_3 + q_1 q_2) & q_0^2 + q_2^2 - q_1^2 - q_3^2 & 2(-q_0 q_1 + q_2 q_3) \\ 2(-q_0 q_3 + q_1 q_3) & 2(q_0 q_1 + q_2 q_3) & q_0^2 + q_3^2 - q_1^2 - q_2^2 \end{pmatrix}.$$

The target function (1) is to be minimized with respect to the four quaternion components. As demonstrated in previous work [9], this constrained minimization can be mapped onto an eigenvector problem of the form $\mathbf{M}\boldsymbol{q} = \lambda\boldsymbol{q}$, where $\mathbf{M} \equiv \mathbf{M}(\{x_\alpha, x'_\alpha\})$ is a positive semi-definite matrix related to the target function. The solution of this kind of problem consists of four eigenvalues, $\lambda_j (j=1,\ldots,4)$, which coincide with the errors in the superposition fit described by the target function. The quaternion corresponding to the smallest eigenvalue, $\lambda_1 = \lambda_{\min}$, is the solution for the optimal fit which leads to the superposition of the two planes and, hence, it gives a description of the relative orientation of $\{x'_\alpha\}$ with respect to $\{x_\alpha\}$. The largest eigenvalue, $\lambda_4 = \lambda_{\max}$, describes, in contrast, the "worst"

superposition and gives the *maximal* Euclidean distance between the two peptide planes. Through λ_{max}, it is possible to define the first ScrewFit parameter, which is the unique orientational distance between two consecutive peptide planes,

$$\Delta_\Omega = \sqrt{\frac{\sum_{\alpha=1}^{3} \omega_\alpha (x_\alpha - x'_\alpha)^2}{\lambda_{max}}}. \qquad (2)$$

One notes that $0 \leq \Delta_\Omega \leq 1$.

The second parameter is radius of the screw motion,

$$\rho = \frac{|t_\perp|}{2} \sqrt{1 + \cot^2(\phi/2)}. \qquad (3)$$

It is derived from Chasles' theorem, which states that any rigid-body displacement (like the superposition of two consecutive peptide planes) can be described by a rotation around an axis passing through a reference point, which may be located outside the rigid body, and a translation along the rotation axis. Here $t_\perp$ is the component of the distance vector $\boldsymbol{t} = \overline{CC'}$, which is orthogonal to the rotation and translation axis n of the screw motion, and ϕ is the rotation angle. Both n and ϕ are obtained through the relation $\boldsymbol{q} = \{\cos(\phi/2), \sin(\phi/2)n_x, \sin(\phi/2)n_y, \sin(\phi/2)n_z\}$, where $\boldsymbol{q}$ is the quaternion describing the optimal rotation.

The straightness σ at residue i is defined by

$$\sigma_i = \mu_i^T \cdot \mu_{i+1}, \qquad (4)$$

where μ_i is given by

$$\mu_i = \frac{\boldsymbol{R}_{i+1}^\perp - \boldsymbol{R}_i^\perp}{|\boldsymbol{R}_{i+1}^\perp - \boldsymbol{R}_i^\perp|}. \qquad (5)$$

The vector $\boldsymbol{R}_i^\perp$ in Eq. (5) locates the point, on the helix axis, which is closest to the C-atom of the ith peptide plane. One has (the residue index is omitted) $\boldsymbol{R}_\perp = \boldsymbol{R}_C + u_\perp$, where $u_\perp = 1/2(u_\perp + \cot(\phi/2)n \times \boldsymbol{t})$. One recognizes that $\rho = |u_\perp|$.

The radius ρ (see Eq. (3)) is related to the distances between the C-atoms, in the reference and target peptide planes, and the local axis of screw motion. The radius ρ is a measure of the local curling of the backbone conformation. In a flat backbone conformation, like an extended β-strand, ρ is close to zero ; when the local backbone conformation is curled, as in the case of α-helices and β-turns, ρ increases. The maximum observed values usually do not exceed 0.3 [9,10].

Straightness σ is the scalar product between the unit vectors of the axis of screw motion, relative to four consecutive peptide planes, it gives information about local curvatures or kinks of a protein backbone tract.

It is worth noting here that both ρ and σ, defined as in Eqs. (3) and (4), give properties intrinsically related to the pair of consecutive peptide planes and should not be associated only to one residue. This fact must be remembered when interpreting the ScrewFit profiles shown in this work.

The comparison of ScrewFit profiles of different NAs is performed through the punctual differences along the sequence axis. This type of comparison is possible only because of the absence of insertions or deletions in the multi-alignment of the corresponding sequences. In the opposite case, comparison is possible only on limited regions where this condition is still verified.

The positive differences in the radius of screw motion (ρ) and the orientational distance (Δ_Ω), indicate a change toward a more curled conformation of the backbone, whereas any deviation from zero of the straightness (σ) is caused by a kink (if located in one or two residues) or a smoother curvature (if more than two residues are involved) in one of the two main chains.

2. Results

2.1. Oseltamivir binding to group-1 NAs

The comparative analysis of the ligand-free against the oseltamivir-bound open and closed conformations of NA1 indicates that there
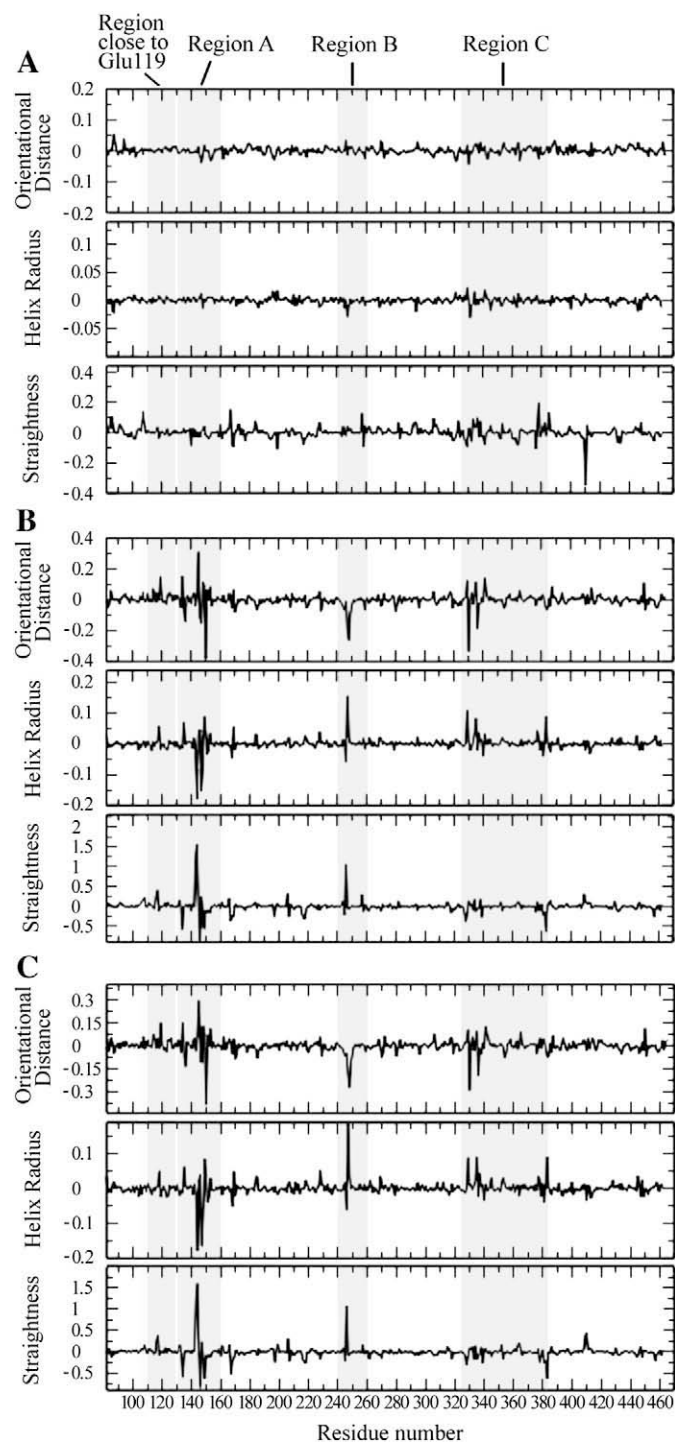

Fig. 2. Screw-Fit parameter differences between the free and oseltamivir-bound open NA1 conformations (Panel A), the free and oseltamivir-bound closed NA1 (Panel B), and oseltamivir-bound open and oseltamivir-bound closed NA1 conformations (Panel C). In both panels, regions A, B, C and Glu119 are highlighted by gray stripes. The positive differences in the radius of screw motion (ρ) and the orientational distance (Δ_Ω), indicate a change toward a more curled conformation of the backbone, whereas any deviation from zero of the straightness (σ) is caused by a kink (if located in one or two residues) or a smoother curvature (if more than two residues are involved) in one of the two main chains.

is not a remarkable difference between the ligand-bound open conformation and the ligand-free structure of NA1, while a significant difference is observed by comparison of the drug-free enzyme and the oseltamivir-bound closed conformation (Fig. 2). The changes found between the two NA1 oseltamivir-bound structures depend on different concentrations (20 μM and 0.5 mM, respectively) of oseltamivir and on different times of crystal soaking (30 min and 3 days, respectively) [11]. As a whole, these observations indicate that oseltamivir binding induces a structural shrinking of NA1, mainly localized just in few regions.

Fig. S3 report the ScrewFit profiles differences among NA8 ligand-free, open and closed conformations, showing that the ScrewFit parameters profiles are quite similar to the NA1 (Fig. 2).

The major structural changes, in both NA1 and NA8, are located in three regions: Arg130-Ser160 (region A; also named 150-loop, see [11]), Val240-Gly260 (region B), and Asp330-Glu385 (region C). The inspection of the amino acid sequence multi-alignment indicates that these regions comprise highly conserved residues involved in ligand binding Glu, and Arg in region A, Ser, and Ala in region B, and Arg in region C (Fig. S1). Regions A and B are characterized by patterns of highly conserved residues, whereas in region C there is more variability. Patterns of mutations in these three regions differentiate group-1 and group-2 NAs, and are responsible for the different oseltamivir binding behavior (see below).

In addition to the regions mentioned above, small conformational change(s) are found also in a narrow region close to Glu119, which is located at the NA1 active site (Fig. 3A). Although this residue appears to interact with oseltamivir in group-1 and group-2 NAs in a similar fashion, its geometry is slightly affected by the open-to-close conformational transition [11]. The variation of the ScrewFit parameters (see Fig. 2) suggests that the NA1 open-to-closed transition parallels with the shift of the Glu119 residue towards Arg118; this could induce a small bending of the Phe115-Cys124 β-strand as indicated by the value of straightness parameter between Ile117 and Glu119.

In region A of NA1, the oseltamivir-induced structural difference(s) distinguishing the open to the closed conformations entail(s) the reduction of the helical radius of several residues and the increase of
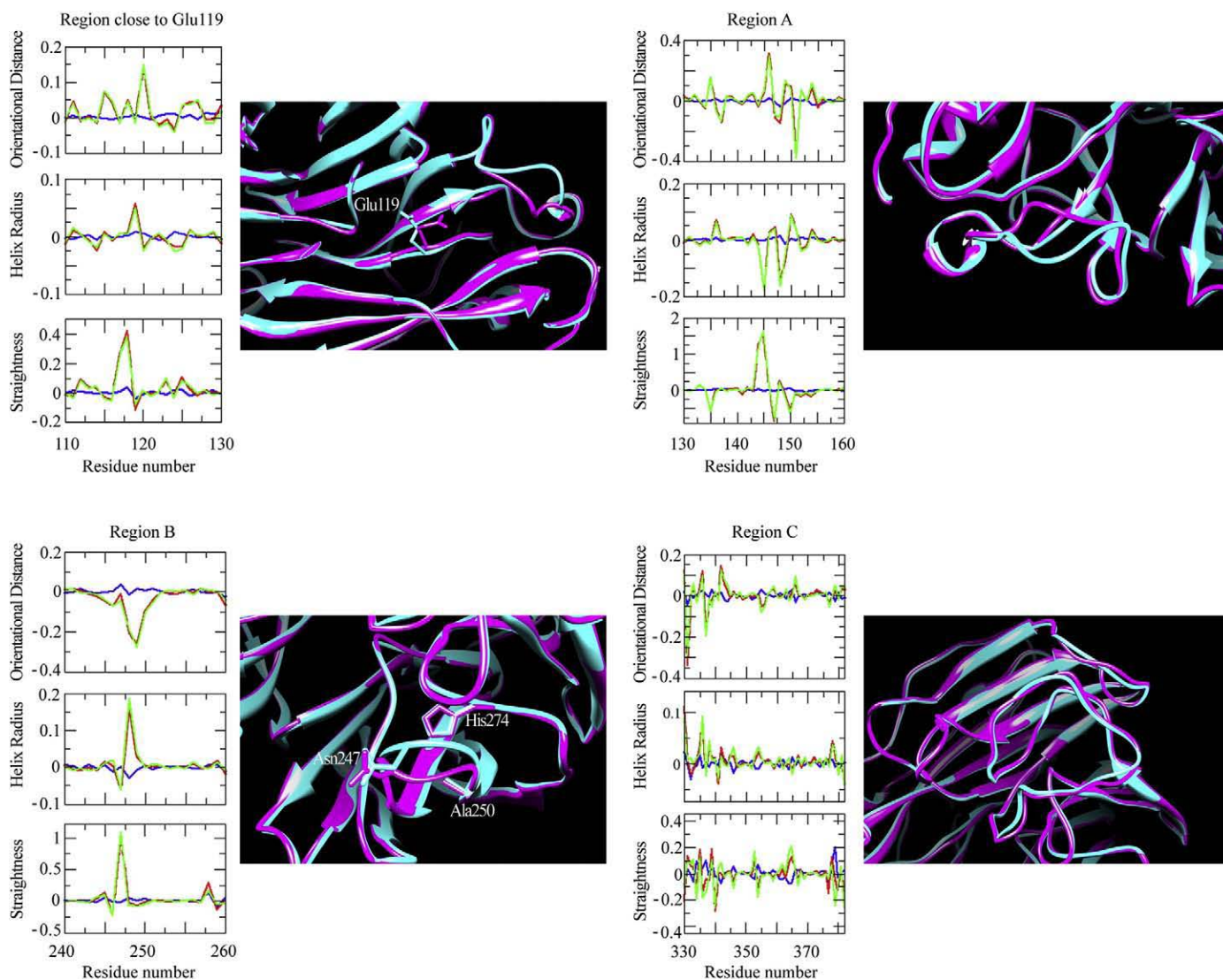

Fig. 3. Comparison between the free, open and closed structures of NA1. ScrewFit difference plots are NA1 free minus NA1 open (blue), NA1 free minus NA1 closed (red), and NA1 open minus NA1 closed (green). The NA1 structure in closed conformation is shown in magenta, while the open structure is in cyan. For major clarity, the NA1 free structure is omitted from all the structural representations, as it is very similar to NA1 open one. (A) In the region close to Glu119, the residues 115–124 of the closed conformation Glu119 shows an additional bending of the β-strand and its side-chains point towards the active site core. (B) Region A (residues 130–160), it is evident the straight loop structure of the open conformation. (C) Region B (residues 240–260), the amino acid Asn247 moves towards a more compact conformation, bending in the direction of the active site center. (D) Region C (residues 330–385). Pictures were drawn by means of UCSF Chimera [21]. (For interpretation of the references to color in this figure legend, the reader is referred to the web version of this article.)
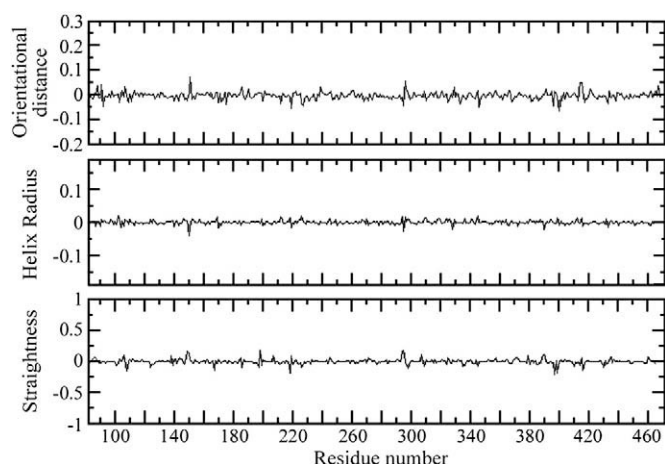
Fig. 4. ScrewFit parameter differences of the ligand-free minus the oseltamivir-bound NA9 structures.

the orientational distance (see Fig. 2). In the closed conformation, the peptide planes of residues Leu140-Arg152 tend to be more distant from the local rotation axis of the screw motion, indicating a change from a flat to a curled conformation. This result can be inferred from the reduction of the radius of the screw motion (ρ) and the corresponding change in the orientational distance (Δ_Ω). The two parameters show that consecutive plans attain different orientations, either lowering their orientational distance (residues Arg130-Ser145) or increasing the latter (region Gly147-Ser160), which demand for a global re-arrangement around the common axis of screw motion. Such a conformational change is also reflected by a remarkable change of the local rotation axis in the sub-region Leu140-Ser145, as shown by the value of the straightness difference which is grater than one, this indicating that the transition between open and closed conformation induces a change of the straightness from a non-negative value to a non-positive one (see Fig. 2). The latter reads as a change of about $\pi/2$ in the direction of the local rotation axis. The differences of the ScrewFit parameters match with the moving of the subregion Ser145-Arg152 to the center of the active site [11] (Fig. 3B).
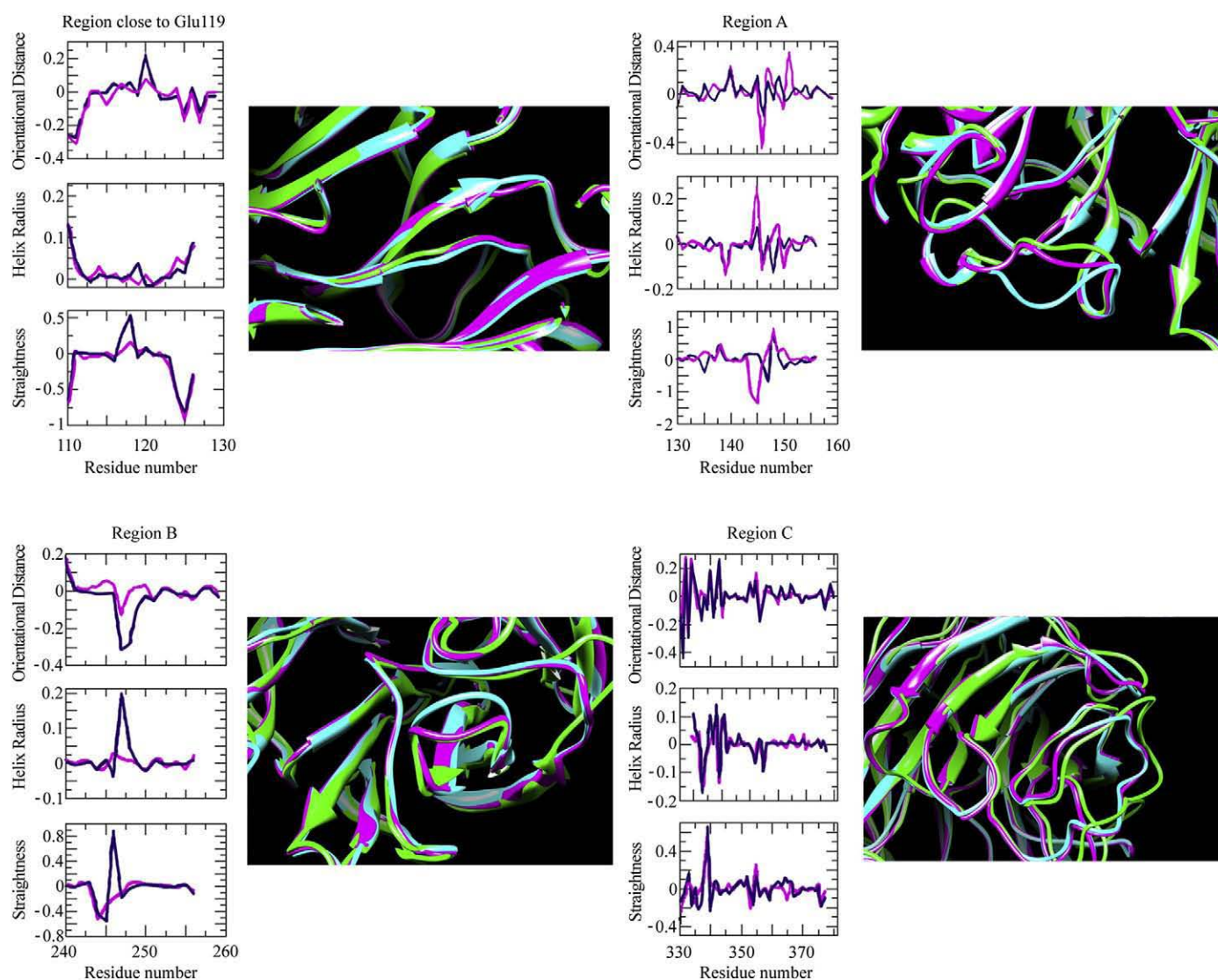

Fig. 5. Comparison between the open and closed structures of NA1 with those of ligand-free NA9. Note that the main differences of the ScrewFit variables of NA1 open form versus NA9 (blue) and NA1 closed conformation versus NA9 (magenta) are in the Glu119, A, B and C regions (see the text). In the three-dimensional representations (right panels) the NA1 open (cyan), NA1 closed (magenta), and ligand-free NA9 (green) structures are shown. Pictures were drawn by means of UCSF Chimera [21]. (For interpretation of the references to color in this figure legend, the reader is referred to the web version of this article.)

Changes of the ScrewFit parameters of region B are similar to those observed in region A, the backbone attaining a more packed conformation around Asn247 as revealed by the positive change in the straightness (close to one), which indicates a kink into the local axis of rotation between residues Asn247 and Gly248. Nevertheless, it is worth noting that here the screw motion helix radius decreases from the open to the closed conformation meaning that the peptide planes assume similar orientations. The extent of this change (~0.1) shows that peptide planes between residue Asn247 and Gly248 adopt a β-turn-like configuration in the closed oseltamivir-bound NA1. The variation in the NA1 structure involves Ala250, which in group-1 NAs makes an hydrogen bond with His274 (Fig. 3C). His274 is known to be the site of the critical mutation His274Tyr, which leads to high resistance of group-1 NAs against oseltamivir [15]. Interestingly, the open-to-closed transition induces a slight change in the length of the hydrogen bond between residues His274 and Pro245 (Fig. 3C). Moreover, the hydrogen bond between residues Gln249 and Ala270 is also affected by the open-to-closed conformational transition, shortening from 3.25 Å to 2.97 Å.

In contrast, oseltamivir binding does not alter significantly the direction of the screw motion axis in region C through the open-to-closed transition; indeed, the difference-plot of straightness parameter is quite flat in this region (Fig. 3D). Nevertheless, this region presents several variations in the orientation of the peptide planes as suggested by changes of the orientational distance and helix radius parameters (see Fig. 2). The latter undergo, between residue Asp330 and Pro340, similar variations as in region B. The rest of local changes in region C are dependent on structural modifications of the intra-chain hydrogen bonds, indeed, they are correlated to changes in the orientation of residues located in the outer protein surface [11].

2.2. Oseltamivir binding to group-2 NAs

Here we will show the effects of oseltamivir binding to a representative member of group-2 NAs. Fig. 4 shows the difference ScrewFit profile of native NA9 minus the enzyme:oseltamivir complex. Oseltamivir binding does not induce structural change(s) in this group-2 NA. This result agrees with the fact that oseltamivir was designed to optimally adapt to group-2 NAs [16].

2.3. Comparison between NA1 and NA9 binding with oseltamivir

In Fig. 5 are reported the difference ScrewFit plots of the open and closed configurations of NA1 minus the ligand-free structure of group-2 NA9. These difference plots are focalized on the regions where major structural changes have been found by the intra-group ScrewFit differences plot (Figs. 2 and 3). This analysis is suggested by the observation that the structure of group-1 NAs tends to resemble that of group-2 upon oseltamivir binding [11]. Following this statement, it would be expected a zero difference ScrewFit plot for the NA1 closed conformation minus ligand-free NA9. Although very similar, our results show that in regions A, B, and C both the open and the closed configuration of NA1 are characterized by variations of the ScrewFit parameters with respect to the NA9 configuration.

The region close to the Glu119 seems to confirm a better super-position of oseltamivir-bound NA1 closed conformation with NA9 free in respect to NA1 open conformation as observed in [11] (Fig. 5A).

In Region A, differences are observed at sites Leu139-Leu140 and Ser145-Arg152, indicating that this region is influenced by oseltamivir binding to group-1 NAs. In particular, residues Gly147 and Arg152 change their configuration through the open-to-closed transition (Fig. 5B). Indeed, in the closed state, they assume a conformation similar to the one in NA9. Nevertheless, in the same region some discrepancies between NA1 closed conformation and NA9 are still present. In particular residues Ser145 and Asp151 shows drastically different backbone conformations in the NAs. This local difference is

also confirmed by the direct visual comparison of the structures shown in Fig. 5B. In Region B, there are pronounced deviations of all three ScrewFit parameters, at the site of the catalytically relevant Ser246. This deviation almost disappears in the NA1 closed conformation (Fig. 5C). In Region C, although the pattern of structural differences is more confused, any significant change seems to differentiate the open and the closed configurations of NA1 in respect to the ligand-free NA9 (Fig. 5D).

3. Discussion and conclusions

The drug-dependent 'induced fit' transition of group-1 to group-2 NAs observed by Russell and coworkers [11], is confirmed and refined here by using the ScrewFit algorithm developed for quantitative molecular structure comparison [8–10]. Indeed, when crystals of NA1 are incubated with oseltamivir a transient open conformation different from that of the drug-free form and from that of the final stable oseltamivir-bound derivative is observed. In turn, the ligand free NA1 and NA9 structure are different, but the final stable oseltamivir-bound NA1 and NA9 conformations are similar. When the oseltamivir-mediated open-to-closed transition in NA1 and NA8 takes place, both Glu119 and Asp151 move toward the bound oseltamivir (Fig. 3). Nevertheless, some significant differences between the oseltamivir-bound group-1 and group-2 are pinpointed by ScrewFit (Fig. 5) and refine the results reported in [11].

Indeed, although the reported 'induced fit' is evident from Figs. 2 and 3, all regions present some sites with an opposite or neutral behavior in respect to this transition. In particular, the residue Asp151, which is known to interact with substrate, clearly assume different backbone configuration in the NA1 closed conformation and in NA9. These results show that the open-to-closed transition does not correspond to a homogeneous 'induced-fit' of group-1 to group-2 NAs [11,16] and reveal a more complex adaptation of the whole three-dimensional structure. Another important clue comes from Fig. 4, where it is shown that NA9 structure is essentially unaffected by oseltamivir binding, suggesting that drug-binding has some thermo-dynamic optimality. It is worth noting that different studies were able to define the active site "geography" of NAs and the location of the residues that recognize the substrate [17–20] (i.e., Arg118, Glu119, Asp151, Arg152, Trp178, Ile222, Arg224, Glu227, Ala/Ser246, Glu276, Glu277, Arg292 and Arg371) (Fig. S1, bold characters). Interestingly, most of the small kinks in the difference plots refer to these residues. These small structural changes could be further exploited in more refined analyses by the ScrewFit algorithm, especially in respect to the minor discrepancies found between NA1 and NA8.

Moreover, it is worth to note that all results from the direct NA1 and NA9 comparison (Fig. 5), have been reported here only qualitatively but they can also be used in a more quantitative manner as a measure of the local discrepancies between different conformations.

The difference plots of the open (induced by 20 μM oseltamivir) and closed (induced by 0.5 mM oseltamivir) configurations of NA1 minus ligand-free structure indicate that at mild inhibitor concentrations there are local distortions not only in the region of the 150-loop [11], but also at residues Val240-Ala250, in the Asp330-Pro340 region and close to residues Pro380 and Phe410 (Fig. 2). Amino acid mutations taking place in these regions, involved in ligand recognition, may modulate drug-binding.

These results confirm and complete the perspectives suggested in [11] and [16] about the design of new antiviral drugs in respect to the effects of inhibitors on the whole structure of NAs. The ScrewFit analysis, although related only on backbone conformational changes, proved to be useful in the evaluation and refinement of crystal-lographic results. Moreover it seems to be potentially relevant also in the assessment of protein structural homology, both locally and globally.

From a structural point of view, present results raise the basic question whether group-1 NAs are more rigid than group-2 enzymes in oseltamivir binding and which role the variability of the regions flanking the active site plays in respect to the flexibility of NAs. Although answering to this kind of questions is not possible through a static analysis, and would require kinetic experiments and dynamic simulations, it is reasonable to assume that, through patterns of function conserving mutations, viral proteins explore not only structural possibilities, but also dynamical repertoires. This hypothesis seems to be confirmed by a preliminary molecular simulation made on ligand-free and oseltamivir-bound NA1 [20], showing that NA1 could explore an ensemble of conformations, same of them even more squashed than the closed or wider than the open one. Therefore, important clues could emerge from the ScrewFit analysis of the NA4 and NA5 structures ligand-free and oseltamivir-bound, when available. Additionally, it would be interesting to have further comparative molecular dynamics simulations of NA1 (or NA8) and NA9, with the aim of checking if phylogenetical distances correspond to different dynamical behaviors.

Acknowledgments

Appendix A. Supplementary data

Supplementary data associated with this article can be found, in the online version, at doi:10.1016/j.bpc.2009.01.004.

References

[1] T. Horimoto, Y. Kawaoka, Pandemic threat posed by avian influenza A viruses, Clin. Microbiol. Rev. 14 (2001) 129–149.

[2] R. Webster, W. Bean, O. Gorman, T. Chambers, Y. Kawaoka, Evolution and ecology of influenza A viruses, Microbiol. Rev. 56 (1992) 152–179.

[3] R. Fouchier, V. Munster, A. Wallensten, T. Bestebroer, S. Herfst, D. Smith, G. Rimmelzwaan, B. Olsen, A. Osterhaus, Characterization of a novel influenza A virus hemagglutinin subtype (H16) obtained from black-headed gulls, J. Virol. 79 (2005) 2814–2822.

[4] E. De Clercq, Antiviral agents active against influenza A viruses, Nat. Rev. Drug Dis. 5 (2006) 1015–1025.

[5] A.C. Hurt, P. Selleck, N. Komadina, R. Shaw, L. Brown, I.G. Barr, Susceptibility of highly pathogenic A (H5N1) avian influenza viruses to the neuraminidase inhibitors and adamantanes, Antiviral Res. 73 (2007) 228–231.

[6] Q. Mai Le, M. Kiso, K. Someya, Y.T. Sakay, T. Hien Nguyen, H.L. Khan Nguyen, N. Dinh Pham, H. Ha Ngyen, S. Yamada, Y. Muramoto, T. Horimoto, A. Takada, H. Goto, T. Suzuki, Y. Suzuki, Y. Kawaoka, Isolation of drug-resistant H5N1 virus, Nature 437 (2005) 1108.

[7] C. Kim, W. Lew, M. Williams, H. Liu, L. Zhang, S. Swaminathan, N. Bischofberger, M. Chen, D. Mendel, C. Tai, W. Laver, R. Stevens, Influenza neuraminidase inhibitors possessing a novel hydrophobic interaction in the enzyme active site. Design, synthesis, and structural analysis of carbocyclic sialic acid analogues with potent anti-influenza activity, J. Am. Chem. Soc. 119 (1997) 681–690.

[8] G. Kneller, Superposition of molecular structures using quaternions, Mol. Simul. 7 (1991) 113–119.

[9] G.R. Kneller, P.A. Calligari, Efficient characterization of protein secondary structure in terms of screw motions, Acta Crystallogr. D 62 (2006) 302–311.

[10] P.A. Calligari, G.R. Kneller, ScrewFit: a novel approach for continuum protein secondary structure assessments, (in preparation).

[11] R. Russell, L. Haire, D. Stevens, P. Collins, Y. Lin, G. Blackburn, A. Hay, S. Gamblin, J. Skehel, The structure of H5N1 avian influenza neuraminidase suggests new opportunities for drug design, Nature 443 (2006) 45–49.

[12] H. Berman, J. Westbrook, Z. Feng, G. Gilliland, T.N. Bhat, H. Weissig, I. Shindyalov, P. Bourne, The protein data bank, Nucleic Acids Res. 28 (2000) 235–242.

[13] J.N. Varghese, V.C. Epa, P.M. Colman, Three-dimensional structure of the complex of 4-guanidino-Neu5Ac2en and influenza virus neuraminidase, Protein Sci. 4 (1995) 1081–1087.

[14] J.N. Varghese, P.W. Smith, S.L. Sollis, T.J. Blick, A. Sahasrabudhe, J.L. McKimm-Breschkin, P.M. Colman, Drug design against a shifting target: a structural basis for resistance to inhibitors in a variant of influenza virus neuraminidase, Structure 6 (1998) 735–746.

[15] H.L. Yen, L.M. Herlocher, E. Hoffmann, M.N. Matrosovich, A.S. Monto, R.G. Webster, E.A. Govorkova, Neuraminidase inhibitor-resistant influenza viruses may differ substantially in fitness and transmissibility, Antimicrob. Agents Chemother. 49 (2005) 4075–4084.

[16] M. Luo, Antiviral drugs fit for a purpose, Nature 443 (2006) 37–38.

[17] V. Stoll, K.D. Stewart, C.J. Maring, S. Muchmore, V. Giranda, Y.G. Gu, G. Wang, Y. Chen, M. Sun, C. Zhao, A.L. Kennedy, D.L. Madigan, Y. Xu, A. Saldivar, W. Kati, G. Laver, T. Sowin, H.L. Sham, J. Greer, D. Kempf, Influenza neuraminidase inhibitors: structure-based design of a novel inhibitor series, Biochemistry 42 (2003) 718–727.

[18] T. Wang, R.C. Wade, Comparative binding energy (combine) analysis of influenza neuraminidase–inhibitor complexes, J. Med. Chem. 44 (2001) 961–971.

[19] G.T. Wang, Y. Chen, S. Wang, R. Gentles, T. Sowin, W. Kati, S. Muchmore, V. Giranda, K. Stewart, H. Sham, D. Kempf, W.G. Laver, Design, synthesis, and structural analysis of influenza neuraminidase inhibitors containing pyrrolidine cores, J. Med. Chem. 44 (2001) 1192–1201.

[20] RE. Amaro, D.D. Minh, L.S. Cheng, W. Lindstrom, A. Olson, J. Lin, W. Li, J. McCammon, Remarkable loop flexibility in avian influenza n1 and its implications for antiviral drug design, J. Am. Chem. Soc. 129 (2007) 7764–7765.

[21] E. Pettersen, T. Goddard, C. Huang, G. Couch, D. Greenblatt, E. Meng, T. Ferrin, UCSF Chimera — a visualization system for exploratory research and analysis, J. Comput. Chem. 25 (2004) 1605–1612.